PRESTRESS LOSS BEHAVIOR OF HIGH-STRENGTH SELF-CONSOLIDATING CONCRETE GIRDERS SUBJECTED TO ELEVATED COMPRESSIVE FIBER STRESSES

Jared E. Brewe, Missouri University of Science and Technology, Rolla, MO
John J. Myers, PhD, PE, Missouri University of Science and Technology, Rolla, MO
Jim Myers, PE, Coreslab Structures, Inc., Marshall, MO

ABSTRACT

Design codes limit the extreme compressive fiber stress of prestressed concrete members to 60% of the concrete strength. While the purpose of this limit is to address serviceability, this restriction limits the capability of the materials. For this study, six prestressed girders were produced with high-strength self-consolidating concrete and were subjected to elevated compressive fiber stress levels ranging between 65% and 84% of initial concrete strength at prestress release. Time dependent concrete strains were measured using a DEMEC mechanical strain gage, with a focus on drying creep behavior and its relationship to prestress losses. It is shown that current AASHTO loss prediction methods developed for high-strength concrete overestimate losses on the order of 20%, whereas older methods developed for normal strength concrete produced more accurate results.

Keywords: prestress losses, self-consolidating concrete, high-strength concrete

INTRODUCTION

High-Strength Concrete (HSC) has become ordinary in the transportation industry because of its beneficial economical and material properties. HSC is advantageous since it reduces material requirements, permits longer girder spans and allows for increased girder spacing; thereby reducing material and total bridge cost. Over the past few years, Self-Consolidating Concrete (SCC) has gained increased use and acceptance in the US due to the reduced potential for segregation, voids and surface defects. SCC can significantly reduce and even eliminate the need for vibration due to the availability of new admixtures, and therefore reduces fabrication time and labor costs. Due to these advantages, SCC is becoming the material of choice for the precast industry as numerous research studies in recent years have studied the material and mechanical properties of SCC for use in precast members. The combination of the performance characteristics of SCC with the engineering properties of HSC will produce a cost effective material for the construction industry.

The design of prestressed concrete members requires accurate prediction of the force in the prestressing strands, which is reduced over time by prestress losses. In prestressed members these losses primarily occur from: elastic shortening, creep, and shrinkage of concrete and relaxation of steel. Of these four losses, only elastic shortening of concrete is not time dependent. Also, the relaxation of steel is the only loss without a corresponding change in strain. The losses related to concrete behavior can be affected by many factors including mix design, strength, curing environment, exposure during service life, and age at loading.

Several stress checks are performed in prestressed concrete design to avoid over-stressing the concrete. The first check is performed immediately after transfer of prestress, with checks performed for both the compression fibers and tension fibers. These stresses must be controlled to prevent crushing of concrete in compression and cracking in tension. Under service loads, excessive fiber stresses may lead to serviceability problems due to creep and micro-cracking. Design codes use allowable limits to control these stresses to ensure adequate design, but the basis for these limits are not well defined.

Therefore, the purpose of this research program was to improve prestress loss prediction and explore the prestress loss behavior of SCC members subjected to fiber stresses in excess of the allowable limits. For this investigation the extreme concrete fiber in compression was stressed to between 65% and 84% of the initial compressive strength (f_{ci}'). Strain measurements were taken over the length of the beam at regular time intervals for prestress loss estimation and will be compared to available prediction methods.

BACKGROUND

The use of HSC in concrete structures has a long history and its application in precast concrete is becoming quite common. While this material had been used since the early 1980's its application in bridge structures, specifically prestressed members, was delayed due to uncertainties in design provisions. During the mid to late 1990's numerous projects

demonstrated the applicability of this material to prestress concrete members. The foremost project was the Louetta Road Overpass in Houston, Texas, a bridge constructed in 1997 utilizing HSC in nearly every aspect[1]. Since that time the specification of HSC in prestressed members has grown greatly towards its near universal application today.

SCC has been utilized in Japan since the early 1990's with applications observed in bridge, building, and tunnel structures[2]. The desire to specify SCC has grown in the US due its performance characteristic in the fresh state. Since SCC can virtually eliminate the need for vibration, there is a great interest in exploring its use in prestressed members. While the fresh properties are beneficial, the effect on hardened properties is not fully understood. Some studies have shown variations in mechanical property behavior of SCC compared to conventional HSC mixtures in the 8 to 12 ksi (55 to 103 MPa) range. Specifically, research results have indicated lower modulus of elasticity (MOE) values for SCC when compared to conventional HSC's[3,4]. This lower MOE is attributed to the fact that lower coarse aggregate contents are often specified and used to obtain the required plastic characteristics of the mix. HSC mixes, as opposed to SCC mixes, often utilize significantly higher course aggregate contents to obtain higher MOE levels for serviceability requirements. This implies that the use of SCC for longer spanning members may require higher levels of pretensioning force to address serviceability related issues for a given mix design with lower MOE values. Recent projects[4,5] have demonstrated the applicability of SCC to prestressed concrete members and have shown little difference between the overall performance of SCC members and normal HSC members.

PRESTRESS LOSS PREDICTIONS

As mentioned above, the design of prestressed concrete members requires accurate prediction of the force in the prestressing strands, which is reduced over time by prestress losses. A variety of methods are available for prestress loss prediction, each falling into three categories: total lump sum estimates, rational approximate methods, and detailed time-dependent analyses. Most of these methods are presented in the A*merican Association of State Highway and Transportation Officials (AASHTO) Load and Resistance Factor Design (LRFD) Bridge Design Specification*[6], the *Precast/Prestressed Concrete Institute (PCI) Design Handbook*[7] and the *PCI Bridge Design Manual*[8]. Several methods falling into these three categories are presented below.

The *AASHTO LRFD Specifications* Approximate Estimates method (Section 5.9.5.3) and *PCI Design Handbook* total loss method would fall into the total lump sum estimate category. The *AASHTO LRFD Specifications* method uses a simple equation which will result in a value for the total long-term prestress losses. The *PCI Design Handbook* states that total loss in prestressed members will range from about 25 to 50 ksi (172 to 345 MPa) for normal weight concrete members. While these methods will provide a good benchmark, more refined analyses are used to improve the accuracy of the prediction.

The rational approximate methods determine the value associated with each specific loss from shrinkage, creep, and relaxation separately. The methods falling into this category

would be the *AASHTO LRFD Specifications* Refined Estimates (Section 5.9.5.4) and the *PCI Design Handbook* method which had been described by Zia et al.[9]. Recently, changes were made to the design equations used in the *AASHTO LRFD Specifications* based upon recommendations from the *National Cooperative Highway Research Program (NCHRP) Report 496: Prestress Losses in Pretensioned High-Strength Concrete Bridge Girders*[10]. This project expanded previous design equations to account for the difference in material properties between normal strength concrete and HSC. Another advantage of these methods is the ability to use either the design parameters from prediction equations or parameters measured on samples representative of the member. These parameters would typically include the concrete strength, modulus of elasticity, ultimate shrinkage strain, and ultimate creep coefficient.

Detailed time-dependent analyses will produce the most accurate prediction of prestress losses, but are uncommon due to the complexity of determining those losses. This complexity stems from the need for specific material properties and calculation of incremental deformation history of the member. Some of these methods are presented and referenced in the *PCI Bridge Design Manual*[8].

Recently, several research projects have been performed exploring long-term prestress losses with a significant portion attempting to quantify the effect of HSC and SCC on these losses. The largest project was summarized in the *NCHRP Report 496*[10] with resulting changes to the *AASHTO LRFD Specifications*. A few other projects are observed below.

Erkmen et al.[5] examined time-dependent prestress losses in full-scale SCC girders and found similar results between normal HSC and SCC girders. They also found that the *PCI Design Handbook* loss prediction methods produced results that were approximately 15% higher than measured values, but noted that the results were reasonable and consistent between conventional concrete and SCC girders.

Naito et al.[4] concluded that the *PCI Design Handbook* method overestimated the prestress losses in both SCC and HSC girders. At 28-days the effective prestress was 16% higher in the SCC girder and 13% higher in the HSC girder than the PCI estimates.

Hale et al.[11] studied the prestress loss behavior of girders subjected to increased fiber stresses. They concluded that the Third Edition of the *AASHTO LRFD Specifications*[12] overestimated the prestress losses by roughly 50%. It was found that the *NCHRP Report 496* equations predicted the losses to within an average of 6%. Their results also supported an increase in the allowable compressive stress limits to $0.70f_{ci}'$.

ALLOWABLE STRESS LIMITS

Currently, the *AASHTO LRFD Specifications*[6,12] and *ACI 318 Building Code Requirements for Structural Concrete*[13] limit the extreme fiber stress in compression of concrete immediately after prestress transfer to 60% of the concrete compressive strength ($0.60f_{ci}'$). The *PCI Standard Design Practice*[7] recognizes this limit but states that "Initial compression

is frequently permitted to go higher in order to avoid debonding or depressing of strands. No problems have been reported by allowing compression as high as $0.70f_{ci}'$." Limits also exist for the extreme fiber stress in tension, which combined with the compression stress limits address serviceability of the concrete members and helps to avoid cracking of concrete. An extensive background into stress limits is explored by Huo et al[14] with the reported purpose of the compressive stress limits to control creep deformation and to prevent micro-cracking. When these limits were first developed in the 1950's, concrete material behavior and construction quality were not as advanced as today. Therefore, numerous projects[11,14,15,16] have challenged this limit, typically reaching the same conclusion that this limit is unnecessary and recommending an increase to $0.70f_{ci}'$.

Noppakunwaijai et al.[15] didn't specifically address compressive fiber stresses but proposed a strength design approach. They concluded that these limits at transfer should be eliminated entirely and that the current working stress analysis be replaced with the strength design method. Their proposed code changes recommended a stress of not greater than $0.75f_{ci}'$ if the engineer continues using working stress design.

Birrcher et al.[16] investigated the effect of increasing the allowable compressive fiber stress on live-load performance of prestressed girders. Static testing was performed on various reduced scale cross-sectional shapes with the purpose of measuring the cracking load. They found that the cracking load was overestimated with current design procedures and that overstressing may result in nonlinear material behavior at service loads. They conclude that increasing the limit to a max of $0.70f_{ci}'$ may be possible pending full scale testing results.

EXPERIMENTAL PROGRAM

Six prestressed concrete beams were cast with targeted release stresses between 60% and 80% of the initial concrete strength. Time-dependent prestress losses will be determined from concrete surface strains and compared to predicted values. Material properties, beam designs and instrumentation are described herein.

MATERIALS

Mixture proportions were chosen to represent a Missouri Department of Transportation approved SCC mix used in everyday operations, and are presented in Table 1. From these mix proportions it can be seen that coarse aggregate fraction is 35.1%. This fraction is lower than typical HSC mixes, typically in the range of 40% to 50%, which should result in a lower modulus of elasticity since the coarse aggregate proportion will affect the stiffness.

The beams contained ½ in (12.7 mm) diameter, low-relaxation prestressing strands with a modulus of elasticity of 28,500 ksi (197,000 MPa) conforming to ASTM A416. For structural testing, mild steel conforming to ASTM Grade 60 (414 MPa) was used for shear reinforcement.

Table 1 Mixture Proportions

Material		Description
Cement	799 lb/yd^3	ASTM Type III Portland Cement
Coarse Aggregate	1367 lb/yd^3	Crushed Limestone - ½ inch MAS
Fine Aggregate	1425 lb/yd^3	ASTM C 33 - Natural River Sand
Water	300 lb/yd^3	
HRWR	88 oz/yd^3	ASTM C 494 Type F - Polycarboxalate
Air Entrainment	9 oz/yd^3	ASTM C 260 – neutralized Vinsol Resin
Water-Cementitious Ratio	0.375	

Note: 1 lb/yd^3 = 0.5933 kg/m^3, 1 oz/yd^3 = 38.69 mL/m^3, MAS = maximum aggregate size

BEAM DESIGN

Due to material and space considerations, six reduced scale T-beams were produced for this study. A typical cross section is shown in Figure 1 with cross-sectional properties for all beams are shown in Table 2. All beams were cast simultaneously; therefore the same prestressing layout was used for all members. To achieve higher fiber stresses, the section width was reduced resulting in a smaller area and greater strand eccentricity. As will be shown in the test results, the target compressive strength at release of prestressing was not achieved resulting in higher compressive fiber stresses than anticipated. Thus, the label used for each beam in the following results and discussion will correspond to the actual percentage of concrete fiber stress. The beams were cast to a length of 15 ft (4.57 m) to ensure full development of prestressing and for later structural testing.

The beams were designed with a target compressive strength at release of 8 ksi (55 MPa) and a target 28-day strength of 10 ksi (69 MPa). Since the beams were cast simultaneously it is assumed that material properties are consistent throughout. At different times during placement 4 in x 8 in (100 mm x 200mm) cylinders were cast for quality control. Cylinder

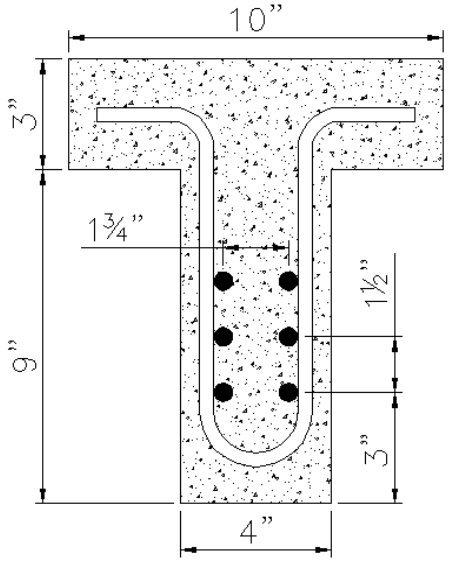

Fig. 1 Representative Cross-Section

Table 2 Beam Cross-Sectional Properties

Target Stress Level	**80**	**75**	**71**	**68**	**64**	**60**
Actual Stress Level	**84**	**79**	**75**	**71**	**68**	**65**
Gross Area, A_g (in^2)	66	69	72	75	78	81
Gross Moment of Inertia, I_g (in^4)	855	895	935	975	1014	1053
Distance from CGC to top fiber, y_t (in)	4.77	4.83	4.88	4.92	4.96	5.00
Distance from CGC to bottom fiber, y_b (in)	7.23	7.17	7.13	7.08	7.04	7.00
Strand Eccentricity, e_p (in)	2.73	2.67	2.63	2.58	2.54	2.50
Distance from top fiber to CGS, d_p (in)	7.50					

Note: CGC = center of gravity of concrete, CGS = center of gravity of steel; 1 in = 25.4 mm

compressive strength was tested at release and 28-days. The modulus of elasticity was determined at 28-days and used to estimate the modulus at release of prestressing.

The strands had a jacking level of 75% of the ultimate strength, resulting in an initial stress before any loss of 202.5 ksi (1396 MPa). Elongation measurements taken before and after jacking were used to determine the initial jacking stress. Since these measurements were taken after chuck seating, the losses associated with seating can be ignored.

INSTRUMENTATION

An estimation of prestress losses is determined from concrete surface strains. These strains were measured using a Detachable Mechanical strain (DEMEC) gauge with an 8 in (200 mm) long gauge length. Stainless steel DEMEC target points were applied to the beams using metal/concrete epoxy. The location of the DEMEC target points for a given section is shown in Figure 2. Target points were placed using the setout bar provided, but initial measurements were used to determine the initial value.

The first target point was placed at approximately 3 in (76.2 mm) from the jacking end with points spaced every 8 in (200 mm) thereafter the entire length of the beam. At each end an additional set of target points were placed at the midpoint of the first to second and second to third points from the end. An additional set was placed at mid-span, with the midpoint of the gauge length exactly at mid-span. This resulted in 25 sets of target points along the length of the beam at the three locations on the web. Along the top of the section, only 3 sets at each end and 3 sets at mid-span were used since these locations were seen as most critical. A representation of DEMEC target point locations for half of the beam is shown in Figure 2.

The critical locations were chosen at mid-span and the ends since this is the location where fiber stresses are typically calculated and checked. The points along the rest of the length

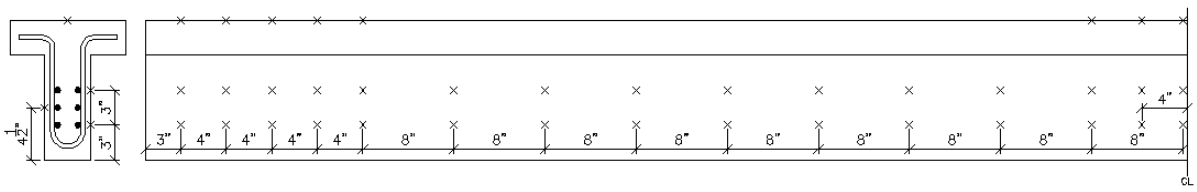

Figure 2 DEMEC Point Layout

can be used to confirm the concrete strains and also used to determine transfer and development length. The points were placed at different depths on the cross section to facilitate development of strain profiles and section curvature. This was done as part of a companion study on the strain distribution effect on prestress losses.

Initial measurements were taken prior to release of prestressing to serve as a reference. Immediately after prestress release, measurements were taken to capture the elastic strain in the member. Follow-up measurements were then taken at 1-day, 7-days, 14-days, and 28-days and subsequently every 28-days thereafter to monitor losses associated with creep and shrinkage of concrete. The difference between the initial reference and current readings is the resulting strain in the concrete between a given set of DEMEC target points. From these measured surface concrete strains an average strain at the center of gravity of the prestressing strands is calculated. The prestress losses can be found by multiplying this average strain by the modulus of elasticity of the prestressing strands.

PRESTRESS LOSS PREDICTION

As mentioned before, there are several methods of prestress loss prediction in use. For this project the *AASHTO LRFD Specifications* Fourth Edition[6] Refined Estimates method, the *PCI Design Handbook*[7] method, and the *AASHTO LRFD Specifications* Third Edition[12] will be used to compare to measured values. The third edition was chosen since that method was developed for normal strength concrete and will provide comparison to the fourth edition published in 2007 which was modified to account for higher strength concrete. Other methods of prestress loss prediction described will not be presented due to the widespread use of these methods.

Prestress losses will be predicted at two stages; immediately after release accounting for the elastic shortening of the member, and at 168 days to match the measurement schedule to account for long term losses due to shrinkage and creep. As mentioned before, the relaxation of steel does not have a corresponding change in strain and since the relaxation of steel is not measured, that loss will be ignored in the following calculations, but for design purposes would need to be included to determine the total prestress losses. Notation used in the following equations can be found at the end of this paper.

The following equation is used to determine elastic shortening losses using both *AASHTO* methods:

$$\Delta f_{pES} = \frac{E_{ps}}{E_{ci}} f_{cgp} \tag{1}$$

This method requires iteration since the value of the prestressing force is used to determine f_{cgp}, which is then reduced by the calculated losses. A direct solution is shown in the commentary of the *AASHTO LRFD Specifications* which can be used to avoid iteration. The equation in the *PCI Design Handbook* is similar to that presented above, with the exception that they assume the prestressing force to be 90% of the initial prestressing force and do not require iteration.

The determination of long-term losses requires the prediction or estimation of the long-term properties of the concrete. The older methods used in the *PCI Design Handbook* and the third edition of the *AASHTO LRFD Specifications* were developed for normal strength concrete and have several assumptions included in their calculations. The newer method attempts to use fewer assumptions to provide increased accuracy, but some inherent assumptions still remain.

The fourth edition of the *AASHTO LRFD Specifications* guides the designer through the process of determining the predicted shrinkage and creep of the concrete; then provides equations for determination of the losses associated with each of them. The equations for determination of shrinkage are:

$$\varepsilon_{sh} = 480 \times 10^{-6} \gamma_{sh} \tag{2}$$

$$\gamma_{sh} = k_{td} k_s k_{hs} k_f \tag{3}$$

Time-Development Factor: $$k_{td} = \frac{t}{61 - 4 f'_{ci} + t} \tag{4}$$

Humidity Factor for Shrinkage: $$k_{hs} = 2.00 - 0.0143 RH \tag{5}$$

Size Factor: $$k_s = \frac{1064 - 94 V/S}{735} \tag{6}$$

Concrete Strength Factor: $$k_f = \frac{5}{1 + f'_{ci}} \tag{7}$$

It can be seen in equation (2) that the ultimate shrinkage is assumed as 480 microstrain. While this value should hold true for the majority of HSC, a larger amount of shrinkage could be expected in this study since the coarse aggregate fraction of the current SCC mix was significantly lower. Previous editions of the *AASHTO LRFD Specifications* used an ultimate shrinkage strain of 560 microstrain for accelerated curing and 510 microstrain for moist curing, but the equations used to determine the influential factors were different. The equations for determination of creep of concrete are:

$$\psi_b = 1.9 k_s k_{hc} k_f k_{td} t_i^{-0.118} \tag{8}$$

Humidity Factor for Creep: $$k_{hc} = 1.56 - 0.008 RH \tag{9}$$

The remaining factors in equation (8) are the same as used for shrinkage prediction. From this equation, it is seen that the ultimate creep coefficient is assumed to be 1.9. Since creep is proportional to applied stress and will vary for different concrete mixtures, the assumed value of this coefficient will affect the accuracy of the predictions.

A transformed section coefficient, K_{id}, is used to account for time-dependent interaction between concrete and bonded steel, which is determined with the following equation:

$$K_{id} = \frac{1}{1 + \frac{E_{ps}}{E_{ci}} \frac{A_{ps}}{A_g} \left(1 + \frac{A_g e_{pg}^2}{I_g} \right) \left[1 + 0.7 \psi_b \right]} \tag{10}$$

Therefore, the losses from shrinkage and creep are determined from the following equations:

$$\Delta f_{pSH} = \varepsilon_{sh} E_{ps} K_{id} \tag{11}$$

$$\Delta f_{pCR} = \frac{E_{ps}}{E_{ci}} f_{cgp} \psi_b K_{id} = \Delta f_{pES} \psi_b K_{id} \tag{12}$$

Since improved equations are used to determine the specific material properties which are then used in the loss prediction equations, this method would be expected to have improved accuracy. Additionally, testing for the specific materials properties used in the prediction equations would eliminate the assumptions and enhance the accuracy.

The PCI Design Handbook method does not require the designer to determine the concrete material properties and provides the following equation for the determination of loss due to shrinkage of concrete:

$$\Delta f_{pSH} = \left(8.2 \times 10^{-6} \right) E_{ps} \left(1 - 0.06 V/S \right) \left(100 - RH \right) \tag{13}$$

Some of the same variables as before are used to account for member size and relative humidity. Similarly, the equation for determination of losses from the creep of concrete is:

$$\Delta f_{pCR} = 2.0 \left(E_{ps} / E_c \right) \left(f_{cir} - f_{cds} \right) \tag{14}$$

From both of these equations the assumptions are evident compared to the method above. The assumed ultimate shrinkage strain is not evident, but the previous method accounts for a larger number of variables in the determination. The same relationship holds for the creep coefficient, but it is apparent that an assumption of 2.0 is used.

The third edition of the AASHTO LRFD Specifications used straightforward equations for the determination of long-term prestress losses. The equations for shrinkage and creep of concrete are:

$$\Delta f_{pSH} = 10.7 - 0.15 \cdot RH \tag{15}$$

$$\Delta f_{pCR} = 12.0 \cdot f_{cgp} - 7.0 \cdot f_{cds} \tag{16}$$

The simplicity of these equations does not allow the designer much control over specific material properties, but can produce reasonably accurate results for some members. Since the concrete mixture proportions used resembled a traditional normal strength concrete mix as compared to a HSC mix, these equations which were developed for normal strength concrete may produce more accurate predictions of prestress losses.

RESULTS AND DISCUSSION

Concrete strength at release of prestressing (3-days) was 7.1 ksi (48.8 MPa). The 28-day strength was found to be 9.0 ksi (62.2 MPa) with a modulus of elasticity of 4635 ksi (31940 MPa). Since the strengths did not reach the target strength, the values of the compressive fiber stresses increased from design as shown in Table 2. Also, the modulus of elasticity of 4635 ksi (31940 MPa) is a great deal lower than anticipated and will affect the prestress loss performance of the members. As was shown above, a reduced value was expected due to the low coarse aggregate fraction but this reduced value was unanticipated. Since the modulus of elasticity was not tested at the release of prestressing, it was determined from a proportional relationship of the square root of the compressive strength, which is similar to the method used for prediction of this modulus.

The development of prestress losses over time is presented in Table 3. These losses were calculated from three measurements at mid-span, which were averaged to the center of gravity of the steel, thus the resulting loss is determined from 9 total measurements. As expected, the members with a greater fiber stress level exhibited an increasing amount of prestress loss due to elastic shortening. Beam 79 would appear to be the only abnormality in the trend. The cause of this irregularity is unclear since the beams were cast from the same batch and the as-cast dimensions are as designed. Following structural testing, further analysis of the beam may offer insight into the cause of the increased losses.

The time-dependent prestress losses exhibit the same trend as elastic losses, with increasing losses from increased fiber stresses. The same irregularity emerges with respect to Beam 79, but Beam 68 also appears to have undergone a larger amount of long-term prestress loss. To provide comparison, the last line in Table 3 presents the ratio of total long-term losses at 168 days to elastic losses. It can be seen that Beams 65, 71, 75, and 84 undergo a relatively similar ratio of long-term losses. Beam 68 exhibits a significantly higher ratio of long-term losses, and Beam 84 resulted in a ratio well below the others.

Table 3 Measured Prestress Losses at Mid-span

Average Measured Prestress Loss at CGS (ksi)							
Designation		**84**	**79**	**75**	**71**	**68**	**65**
Beam Age (Days)	Elastic	28.2	32.6	27.0	26.5	25.5	25.4
	1	34.5	39.3	33.0	32.9	35.7	32.2
	7	42.7	45.2	41.1	39.3	43.4	39.1
	14	48.3	51.7	45.8	45.2	48.0	43.4
	28	52.8	56.5	50.5	49.5	52.3	47.4
	56	59.7	63.7	56.9	55.2	58.3	54.1
	84	63.5	68.0	61.2	60.2	63.5	58.8
	112	64.8	69.6	62.8	61.7	65.8	61.3
	140	65.7	70.8	63.7	62.5	66.8	61.4
	168	66.3	71.1	64.0	63.1	66.8	61.4
$\Delta f_{p168}/\Delta f_{pES}$		**2.35**	**2.18**	**2.37**	**2.38**	**2.62**	**2.42**

Note: Measured losses do not include relaxation of steel, CGS = center of gravity of steel; 1 ksi = 6.89 MPa

Figure 3 presents a visual representation of the reduction in prestressing force over time due to the losses presented in Table 3. The initial prestressing force is noted as 202.5 ksi (1396 MPa). As noted above, the results are similar for all beams except Beam 84 which exhibited larger values at both elastic and long-term and Beam 68 which undergoes a larger amount of long-term losses. Additionally, this plot demonstrates that the majority of prestress losses occur within the first 6 months as the stresses begin to level out between 140 and 168 days.

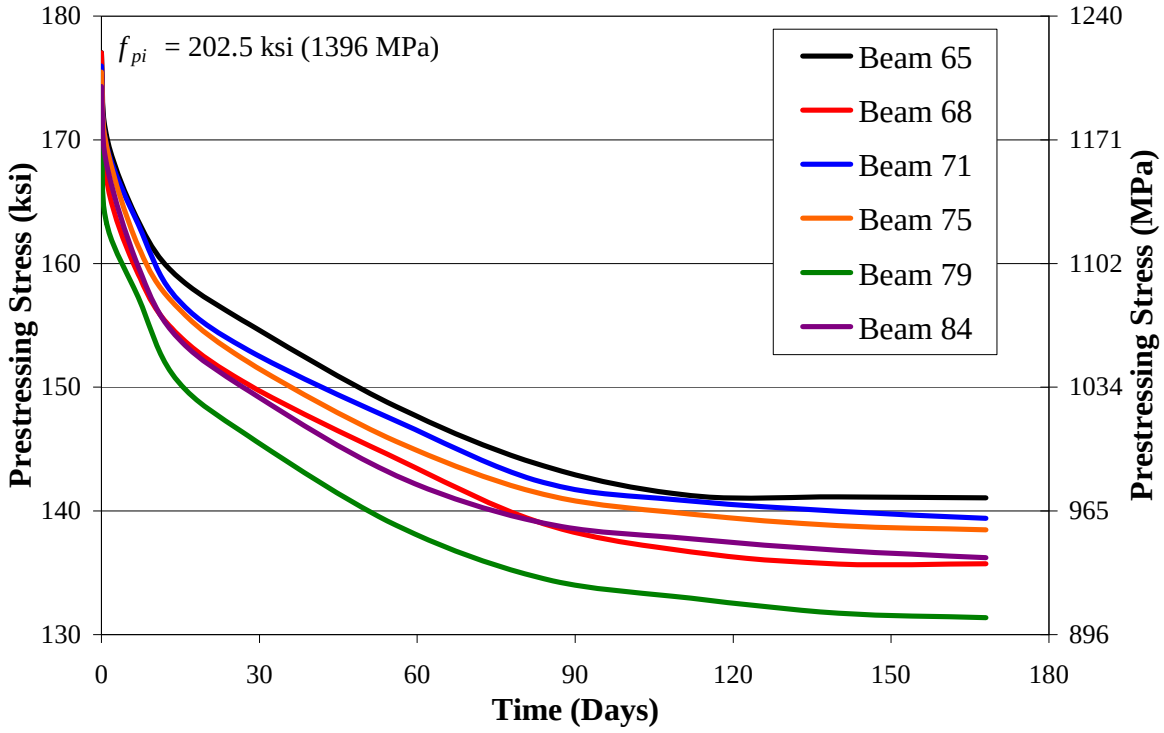

Fig 3 Loss of Prestressing Stress over Time

The comparison of measured and predicted losses are presented in Table 4. The measured elastic losses are underestimated on every beam with the prediction having a greater accuracy at higher fiber stress levels. Since the methods are similar, both prediction methods produce relatively similar results with similar underestimation. Since the only properties used in calculations at this stage are the geometric properties and the elastic modulus of each material, these results were expected to be more accurate.

In regards to long-term losses, the methods produced mixed results. The 2007 AASHTO refined method underestimates the prestress losses for all beams by an average of 22%. The PCI method results in overestimation of all beams by an average of 11%. The third edition of AASHTO produced an average overestimation of 8%. Beam 68 appears to have the most accurate prediction, but is unreliable since as was discussed above it had an irregular amount of long-term losses. It is also apparent that at stress levels closer to current allowable values, the PCI and AASHTO third edition methods produce more accurate results.

Table 4 Comparison between Measured and Predicted Losses (with percent error)

Designation	84	79	75	71	68	65
Elastic Losses (ksi)						
Measured	28.2	32.6	27.0	26.5	25.5	25.4
AASHTO	26.7	25.4	24.1	23.0	22.0	21.1
	-5%	-22%	-11%	-13%	-14%	-17%
PCI	27.7	26.1	24.7	23.4	22.2	21.2
	-2%	-20%	-9%	-12%	-13%	-17%
Total Losses at 168 days (ksi)						
Measured	66.3	71.1	64.0	63.1	66.8	61.4
AASHTO – 4th Ed. Refined Estimates	56.4	54.1	52.0	50.0	48.3	46.6
	-15%	-24%	-19%	-21%	-28%	-24%
PCI	82.3	77.8	73.9	70.3	67.1	64.2
	24%	9%	15%	11%	1%	5%
AASHTO – 3rd Ed.	78.5	74.9	71.5	68.5	65.8	63.3
	19%	5%	12%	9%	-1%	3%

Note: Losses do not include relaxation of steel, 1 ksi = 6.89 MPa

CONCLUSIONS

The following conclusions were drawn from the results of the research study undertaken:

1. Prediction of elastic shortening losses for all beams was less accurate than anticipated. The improved accuracy was expected since the properties used are less variable at early ages, but the results show otherwise.
2. Prestress loss predictions for SCC girders with compressive fiber stresses well above $0.6f_{ci}'$ has shown a large disparity using different methods. Older methods developed for normal strength concrete show slight overestimation, while the newer methods developed for HSC show larger underestimation compared to measured values.
3. Accurate prediction of material properties greatly affects the 2007 AASHTO model. Properly tested and measured ultimate shrinkage strains and creep coefficients would improve prediction accuracy.
4. The last line in Table 3 suggests that higher fiber stress levels will result in a larger proportion of the total long-term losses resulting from elastic shortening.
5. Increasing the fiber stress level to at least $0.70f_{ci}'$ as suggested by others appears to be feasible, pending the results of structural testing.
6. Although these results show improved prediction using the older methods, the authors believe that the 2007 AASHTO method would produce superior results for the majority of projects. This method uses improved equations with fewer assumptions that would normally provide more accurate results.

ACKNOWLEDGEMENT

The authors would like to acknowledge the support from Coreslab Structures, Inc. in Marshall, MO and from the Center for Transportation Infrastructure and Safety (CTIS) at the Missouri University of Science and Technology (formerly the University of Missouri-Rolla) for funding this project. The engineers and personnel at Coreslab Structures, Inc. are acknowledged for their contributions during planning and production. The technician and staff support from the Center for Infrastructure Engineering Studies (CIES) and Department of Civil, Architectural, and Environmental Engineering at the Missouri University of Science and Technology is also acknowledged for their support of the work undertaken in this study.

NOTATION

A_g = gross area of section

A_{ps} = area of prestressing steel

CGS = center of gravity of prestressing steel

e_{pg} = eccentricity of prestressing steel

E_{ps} = modulus of elasticity of prestressing strands

E_{ci} = modulus of elasticity of concrete at release

f_{cgp} = concrete stress at CGS

f_{cds} = concrete stress at CGS due to service dead loads

f'_{ci} = compressive strength of concrete at release

k_f = factor for the effect of concrete strength

k_{hc} = humidity factor for creep

k_{hs} = humidity factor for shrinkage

k_s = factor for the effect of volume-to-surface ratio

k_{td} = time development factor

RH = relative humidity

V/S = volume-to-surface ratio

Δf_{pES} = loss due to elastic shortening

Δf_{pSH} = loss due to shrinkage of concrete

Δf_{pCR} = loss due to creep of concrete

ε_{sh} = concrete shrinkage strain

ψ_b = girder creep coefficient

Table 1. Mixture Proportions

Cer

REFERENCES

1. Myers, J.J.; "Production and Quality Control of High Performance Concrete in Texas Bridge Structures," Dissertation, University of Texas – Austin (1998)
2. Ouchi, M.; Nakamura, S.; Osterberg, T.; Hallberg, S.-E.; and Lwin, M.; "Applications of Self- Compacting Concrete in Japan, Europe and the United States," 2*003 International Symposium on High-Performance Concrete*, Orlando, FL (2003)
3. Schindler, A.K.; Barnes, R.W.; Roberts, J.B.; and Rodriguez, S.; "Properties of Self-Consolidating Concrete for Prestressed Members," *ACI Materials Journal*, V. 104, No. 1, January-February 2007, pp. 53-61
4. Naito, C.J.; Parent, G.; and Brunn, G.; "Performance of Bulb-Tee Girders Made with Self-Consolidating Concrete," *PCI Journal*, V. 51, No. 6, November–December 2006, pp. 72-85
5. Erkmen, B.; Shield, C.K.; and French, C.E.; "Time-Dependent Behavior of Full-Scale Self-Consolidating Concrete Precast Prestressed Girders," *Self-Consolidating Concrete for Precast Prestressed Applications (ACI SP-247)*, American Concrete Institute, Farmington Hills, MI (2007)
6. American Association of State Highway and Transportation Officials, *AASHTO-LRFD Bridge Design Specifications*, Fourth Edition, Washington, DC (2007)
7. Precast/Prestressed Concrete Institute, *PCI Design Handbook, Precast and Prestressed Concrete*, Sixth Edition, Chicago, IL (2004)
8. Precast/Prestressed Concrete Institute, *PCI Bridge Design Manual*, First Edition, Chicago, IL (2000)
9. Zia, P.; Preston, H.K.; Scott, N.L.; and Workman, E.B.; "Estimating Prestress Losses," *Concrete International*, V. 1, No. 6, June 1979, pp. 32-38
10. Tadros, M.K.; Al-Omaishi, N.; Seguirant, S.J.; and Gallt, J.G.; "Prestress Losses in Pretensioned High–Strength Concrete Bridge Girders," *National Cooperative Highway Research Program Report 496*, TRB, National Research Council, Washington DC (2003)
11. Hale, W.M.; and Russell, B.W.; "Effect of Allowable Compressive Stress at Release on Prestress Losses and on the Performance on Precast, Prestressed Concrete Bridge Girders," *PCI Journal*, V. 51, No. 2, March–April 2006, pp. 14-25
12. American Association of State Highway and Transportation Officials, *AASHTO-LRFD Bridge Design Specifications*, Third Edition, Washington, DC (2004)
13. American Concrete Institute (ACI 318-05), *Building Code Requirements for Structural Concrete*, American Concrete Institute, Farmington Hills, MI (2005)
14. Huo, X.; Savage, J.M.; Tadros, M.K.; "Reexamination of Service Load Limit Compressive Stress in Prestressed Concrete Members," *ACI Structural Journal*, V. 92, No. 2, March–April 1995, pp. 199-210
15. Noppakunwaijai, P.; Tadros, M.K.; Ma, Z.; and Mast, R.F.; "Strength Design of Pretensioned Flexural Concrete Members at Prestress Transfer," *PCI Journal*, V. 46, No. 1, January-February 2001, pp. 34-52
16. Birrcher, D.B.; Tuchscherer, R.G.; Mraz, D.; Castro, A.; Bayrak, O.; and Kreger, M.E.; "Effects of Increasing the Allowable Compressive Release Stress of Pretensioned Girders," *2006 Concrete Bridge Conference*, Grapevine, TX, 20 pp